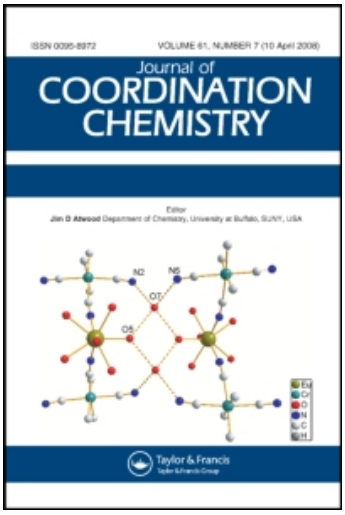

Journal of Coordination Chemistry
Publication details, including instructions for authors and subscription information:
http://www.informaworld.com/smpp/title~content=t713455674

Magnetic properties, infrared spectroscopy, thermal and theoretical studies of oxomolybdenum(V) complexes with 2,2'-bipyrimidine

Delia B. Soria[a]; Montserrat Barquín[b]; Maria J. Gonzalez Garmendia[b]; Guillermina Estiu[c]
[a] Cequinor, Facultad de Ciencias Exactas, Universidad Nacional de La Plata, CC 962, 1900-La Plata, Argentina [b] Grupo de Química Inorgánica, Facultad de Ciencias Químicas, Universidad del País Vasco, Apartado 1072, 20080-San Sebastian, Spain [c] Department of Chemistry and Biochemistry, University of Notre Dame, Notre Dame, IN 46556, USA

To cite this Article Soria, Delia B. , Barquín, Montserrat , Garmendia, Maria J. Gonzalez and Estiu, Guillermina(2008) 'Magnetic properties, infrared spectroscopy, thermal and theoretical studies of oxomolybdenum(V) complexes with 2,2'-bipyrimidine', Journal of Coordination Chemistry, 61: 23, 3815 — 3828
To link to this Article: DOI: 10.1080/00958970802136354
URL: http://dx.doi.org/10.1080/00958970802136354

Journal of Coordination Chemistry
Vol. 61, No. 23, 10 December 2008, 3815–3828

Magnetic properties, infrared spectroscopy, thermal and theoretical studies of oxomolybdenum(V) complexes with 2,2′-bipyrimidine

DELIA B. SORIA*†, MONTSERRAT BARQUÍN‡, MARIA J. GONZALEZ GARMENDIA‡ and GUILLERMINA ESTIU§

†Cequinor, Facultad de Ciencias Exactas, Universidad Nacional de La Plata, CC 962, 1900-La Plata, Argentina
‡Grupo de Química Inorgánica, Facultad de Ciencias Químicas, Universidad del País Vasco, UPV/EHU, Apartado 1072, 20080-San Sebastian, Spain
§Department of Chemistry and Biochemistry, University of Notre Dame, Notre Dame, IN 46556, USA

(*Received 6 January 2008; in final form 3 March 2008*)

Mono- and dinuclear complexes of oxomolybdenum(V) with 2,2′-bipyrimidine (bpym), $MoOCl_3$(bpym) (**1**) as two geometric isomers (**violet** and **brown**), $Mo_2O_3Cl_4(bpym)_2$ (**2**), $Mo_2O_4Cl_2(bpym)_2$ (**3**), and $Mo_2O_2Cl_6(\mu\text{-bpym})$ (**4**), have been prepared and characterized by EPR, electronic, infrared and Raman spectroscopy, thermal analysis and theoretical calculations. Magnetic susceptibilities in the 4.6–290 K range show different magnetic behavior for the MoO^{3+}, $Mo_2O_3^{4+}$ and Mo_2O_2 $(\mu\text{-bpym})^{6+}$ units. The EPR spectra have also been registered. Theoretical calculations converged to two stable isomers named *cis* and *trans* for $MoOCl_3$(bpym), $Mo_2O_3Cl_4(bpym)_2$ and for $Mo_2O_4Cl_2(bpym)_2$ but four isomers for $Mo_2O_2Cl_6(\mu\text{-bpym})$. Based on the theoretical and experimental results for the violet and brown **1**, we assume that both *cis* and *trans* isomers are present in the solid state. This could also explain the existence of two isomers in $Mo_2O_2Cl_6(\mu\text{-bpym})$.

Keywords: 2,2′-Bipyrimidine; Oxomolybdenum(V); Antiferromagnetic dimer; Diamagnetic dimer; Theoretical analysis

1. Introduction

Molybdenum(V) complexes have been studied for their capability of forming monomeric and dimeric compounds with different ligands. In dinuclear complexes, bridges are usually one or two oxygens, two sulfurs or two chlorides. Molybdenum in the +5 oxidation state forms a variety of complexes having either the monomeric MoO or the oxo-bridged Mo_2O_3, Mo_2O_4 structural units, which invariably contain one multiple bonded terminal atom per molybdenum [1–5].

Studies on molybdenum(V) chemistry frequently face difficulty in discerning among the several types of oxygen-bridged dimers that occur. Infrared spectral measurements

*Corresponding author. Email: soria@quimica.unlp.edu.ar

Journal of Coordination Chemistry
ISSN 0095-8972 print/ISSN 1029-0389 online © 2008 Taylor & Francis
DOI: 10.1080/00958970802136354

of metal-to-oxygen multiple bonded systems have been only attained for the compounds in which the oxo ligand is in a terminal position.

In complexes of the general type $[\{Mo(O)(X)\}_2\text{-}(O)_x(S)_{2-x}]$ [X = dithiocarbamate, $S_2CNR_2^-$, or phosphorodithionate $S_2P(OR)_2^-$; $x = 0$–2], the molybdenums are five coordinate and displaced towards the terminal oxide [6]. The possibility of changing coordination number in molybdenum chemistry is of interest in catalysis, as it allows the binding of substrates to molybdoenzymes [7]. Isomerism of Mo complexes has been extensively studied. In 1971, Saha *et al.* [8] reported the isolation of $MoOBr_3Phen$ in two colored forms (red and deep chocolate), associated with *cis* and *trans* stereoisomers; their hydrolysis gave oxo and dioxo bridged dimeric species. Chatt *et al.* [9] reported the synthesis of a series of octahedral molybdenum oxo complexes bearing phosphine ligands; *cis-mer* $Mo\text{–}OCl_2(PMe_2Ph)_3$ has been isolated in both blue and green isomeric forms with slightly different $\nu(Mo{=}O)$ stretching frequencies (blue 954 cm^{-1} and green 943 cm^{-1}) [10]. However, after extensive investigations the existence of several different bond lengths was explained as a crystallographical disorder caused by co-crystallization of the isostructural yellow trichloride complex *mer* $MoCl_3(PMe_2Ph)_3$ as an impurity [11]. Gibson *et al.* [12] have found the conditions required to crystallize each form; the blue form (954 cm^{-1}) is obtained by crystallization from ethanol in the presence of water, whereas the green form (943 cm^{-1}) is obtained in dry solvent.

These different findings prompted us to investigate Mo(V) complexes with different ligands and different kinds of solvents to better understand the influence of ligand and solvent on the chemistry of Mo(V). In this article we describe the synthesis and characterization of a new molybdenum(V) dioxo complex of 2,2′-bipyrimidine, $Mo_2O_4Cl_2(bpym)_2$ and an improved method for the preparations and characterization of $MoOCl_3(bpym)$ (violet and brown), $Mo_2O_3Cl_4(bpym)_2$ and $Mo_2O_2Cl_6(\mu\text{-bpym})$, having respectively the $[MoO]^{3+}$, $[Mo_2O_3]^{4+}$ and $[Mo_2O_2(\mu\text{-bpym})]^{6+}$ units [13]. The complexes contain 2,2′-bipyrimidine as a bidentate ligand or as a bis-bidentate bridge between two Mo atoms (see scheme 1). In the latter, the bpym facilitates weak antiferromagnetic intradimer exchange [14, 15].

Spectroscopic FTIR, Raman and EPR spectra, thermal and magnetic characterization of the complexes are reported. No reliable crystal structure could so far be determined for all the complexes, but the results of theoretical calculations provide better understanding of the solid properties.

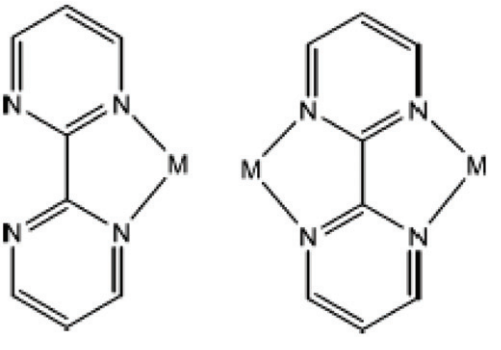

Scheme 1. 2,2′-Bipyrimidine ligand coordinated in a bidentate mode (left) and coordinated in a bis(bidentate) bridging mode (right).

2. Experimental

2.1. *Preparation of complexes*

The Saha and Halder method [3] was followed for the preparation of $(NH_4)_2[MoOCl_5]$.

2.1.1. $MoOCl_3$(bpym) (violet) and $MoOCl_3$(bpym) (brown) (1). The reaction of a solution of bpym (1.92 mmol, 0.30 g) in 20 mL of absolute ethanol with $MoCl_5$ (1.28 mmol, 0.35 g) in 20 mL at room temperature gave a violet precipitate after stirring the mixture at room temperature for 30 min. The precipitate was filtered off, washed with ethanol and dried in air. Yield 99.5%. Anal. Calcd for $C_8Cl_3H_6MoN_4O$ (**violet**) (%): C, 25.52; H, 1.61; N, 14.88. Found: C, 25.57; H, 1.75; N, 14.54.

When 96% ethanol was used instead of absolute ethanol and the stirring maintained at room temperature for 5 h, a **brown** precipitate formed. Yield 99%. Anal. found (%): C, 25.59; H, 1.75; N, 14.84.

2.1.2. $Mo_2O_3Cl_4(bpym)_2$ (violet) (2). The reaction of a solution of bpym (1.92 mmol, 0.30 g) in 20 mL of absolute ethanol with $MoCl_5$ (1.92 mmol, 0.525 g) in 20 mL at room temperature gave a violet precipitate after stirring the mixture at room temperature for 30 min. The precipitate was filtered off, washed with ethanol and dried in air. The same violet powder was obtained from reaction between 1.92 mmol (1.63 g) of $(NH_4)_2[MoOCl_5]$ in 20 mL of absolute ethanol and 1.92 mmol (0.30 g) of bpym in 20 mL absolute ethanol. Yield 98%. Anal. Calcd for $C_{16}Cl_4H_{12}Mo_2N_8O_3$ (%): C, 27.51; H, 1.72; N, 16.05. Found: C, 27.80; H, 2.08; N, 15.5.

2.1.3. $Mo_2O_4Cl_2(bpym)_2$ (orange) (3). The reaction between 1.92 mmol (0.525 g) of $MoCl_5$ or 1.92 mmol (1.63 g) of $(NH_4)_2[MoOCl_5]$ in 20 mL of 96% ethanol and 1.92 mmol (0.30 g) of bpym in 20 mL of 96% ethanol gives an orange powder. Yield 99%. The same result is obtained when the crude μ-oxo complex was washed with 96% ethanol instead of absolute ethanol. Anal. Calcd for $C_{16}Cl_2H_{12}Mo_2N_8O_4$ (%): C, 29.80; H, 1.88; N, 17.40. Found: C, 29.50; H, 2.06; N, 16.12.

2.1.4. $Mo_2O_2Cl_6$(μ-bpym) (brown) (4). Reaction of 1.53 mmol (0.42 g) of $MoCl_5$ in 20 mL of chloroform and 0.76 mmol (0.12 g) of bpym in 20 mL chloroform gave **4** as a brown powder after stirring the mixture at room temperature for 24 h. The precipitate was filtered off, washed with chloroform and dried in air. Yield 97%. Anal. Calcd for $C_8Cl_6H_6Mo_2N_4O_2$ (%): C, 16.14; H, 1.01; N, 9.41. Found: C, 16.43; H, 1.08; N, 9.08.

2.2. *Physical measurements*

C, H and N were analyzed using a Perkin–Elmer 240C elemental analyzer. Visible spectra were recorded on a UV/vis spectrophotometer (Shimadzu UV-300, Hewlett-Packard 8453 diode-array). IR spectra were recorded in the 4000–400 cm^{-1}

range using KBr pellets on a Nicolet FT-IR spectrometer. The Raman spectra were recorded with a Bruker IFS 66 spectrophotometer. Thermal analyses were made with Shimadzu TGA 50 and DTA 50H under oxygen flowing at 50 mL min^{-1}. The heating rates were 5°C min^{-1}. Magnetic measurements were carried out in the 290–4.6 K range with a Manics DSM8 magnetometer equipped with a He continuous-flow cryostat and Drusch EAF 16UE electromagnet. The EPR spectra were recorded with a Bruker ESP 300 spectrometer with a Bruker ER 035 M Gaussmeter, Oxford ITC4 cryostat and HP 5325B frequency counter.

2.3. *Theoretical calculations*

Computational study of the Mo transition metal complexes has been carried out using the density functional theory (DFT) methods implemented in Gaussian 03 [16]. The systems studied herein were subjected to unrestrained energy minimizations using the B3LYP functional [17] with the 6–31 + G* basis set [18] for nonmetal atoms and the Los Alamos effective core potentials (LANL2DZ) [19] for Mo. DFT methods have been shown to reproduce the structural properties of several biologically interesting transition metal centers, and their validity to model ground-state properties is widely accepted [20]. The calculated geometries are contrasted with experimental data and the nature of the singular points addressed through the calculation of the Hessian matrix components. IR frequencies have been calculated by means of the same procedure and have been corrected using 0.9614 as scaling factor [21].

3. Results and discussion

3.1. *Structural characteristics*

The structures of the compounds from the geometry optimization procedure are shown in figure 1. Relevant calculated bond distances are reported in Supplemental Material; all calculated distances and angles are within the range found in other Mo(V) structures containing Mo=O groups, including those with bpym (see below) [22–27] and references therein].

3.2. *Visible spectra*

The visible spectra of the complexes have been determined using nitromethane as solvent. The main electronic transitions are reported in table 1. The values are in good agreement with those reported for related complexes [28].

Both the monomeric and dimeric complexes exhibit two bands close to 500 and 750 nm, which were attributed to $^2B_2 \rightarrow {}^2B_1$ and $^2B_2 \rightarrow {}^2E(I)$ according to the Balhausen-Gray scheme for an octahedral structure [29]. The high intensity of the band at 524 nm in the monomeric violet complex relative to the one in the brown one gives the intense color to the monomeric complex. A third transition around 420–480 nm must be assigned to a L → Mo charge transfer.

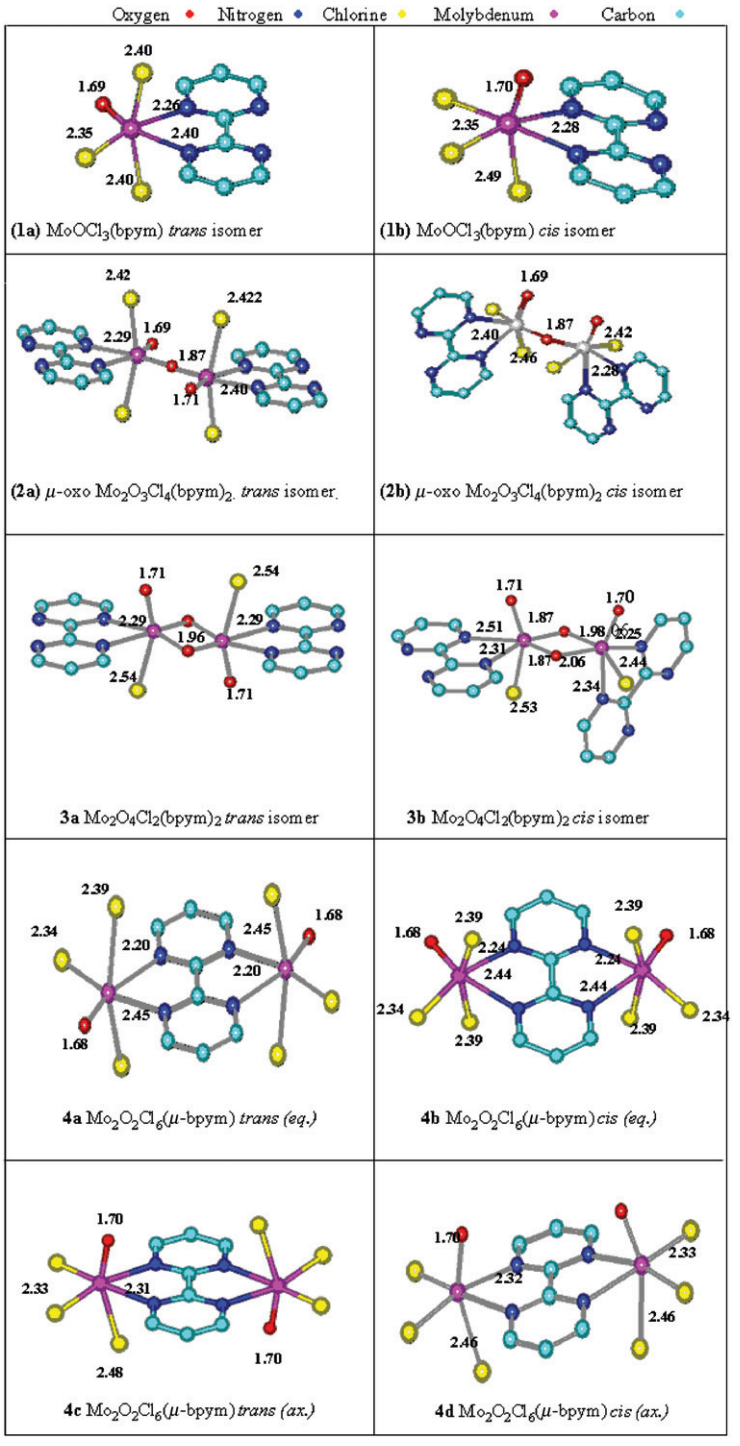

Figure 1. Structures derived from the theoretical calculations. Relevant bond distances are shown. In all cases the geometry optimization converged to two stable isomers (named *cis* and *trans*) but four stable isomers for $Mo_2O_2Cl_6$(μ-bpym). More details are given in the text.

Table 1. Electronic spectra of the $MoOCl_3(bpym)$ **violet** and **brown**, $Mo_2O_3Cl_4(bpym)_2$ $Mo_2O_4Cl_2(bpym)_2$ and $Mo_2O_2Cl_6(\mu\text{-bpym})$ complexes.

Compound	λ_{max} (nm)	ε	Assignments
$MoOCl_3(bpym)$ (**violet**)	420	539	L → Mo (CT)
	524	9901	$^2B_2 \rightarrow {}^2B_1$
	740	170	$^2B_2 \rightarrow {}^2E(I)$
$MoOCl_3(bpym)$ (**brown**)	420	375	L → Mo
	524	277	$^2B_2 \rightarrow {}^2B_1$
	740	123	$^2B_2 \rightarrow {}^2E(I)$
$Mo_2O_3Cl_4(bpym)_2$	431	3376	L → Mo
	525	7341	$^2B_2 \rightarrow {}^2B_1$
	722	983	$^2B_2 \rightarrow {}^2E(I)$
$Mo_2O_4Cl_2(bpym)_2$	420	2137	L → Mo
	–	–	
	–	–	
$Mo_2O_2Cl_6(\mu\text{-bpym})$	478	2018	L → Mo
	623	1776	$^2B_2 \rightarrow {}^2B_1$
	721	1658	$^2B_2 \rightarrow {}^2E(I)$

3.3. *Vibrational spectra and structural characterization*

The main features of the infrared spectra of **1**–**4** are summarized in table 2. The most relevant bands for determination of the structures are those in the 900–1000 cm^{-1} region, associated with Mo=O stretching modes [30].

The two crystalline forms of $MoOCl_3(bpym)$ exhibited slightly different IR spectroscopic properties in the solid. The infrared spectra of both compounds have ν(Mo=O) stretching bands at 977 cm^{-1} in the FTIR spectra and 976 cm^{-1} in Raman spectra, and an additional band at 943 cm^{-1} which is very weak in the **violet** complex, and with higher intensity in the **brown** one.

Calculations found two stable isomers, **1a** and **1b** (figure 1). In **1a** the oxygen lies in the same plane as the bpym ligand, with a Mo=O bond length of 1.69 Å and a calculated Mo=O stretching frequency of 980 cm^{-1}. In **1b**, the oxygen lies out of the bpym plane, with Mo=O distance of 1.70 Å and a calculated stretching ν(Mo=O) of 950 cm^{-1}. In both cases the Mo=O bond lengths (1.69 and 1.70 Å) are within the range found in other Mo(V) structures containing Mo=O groups [28–30 and references therein]. Both structures are almost isoenergetic at the calculation level, with **1a** only 2 Kcal mol^{-1} more stable than **1b**. The optimized geometry is in very good agreement with the X-ray structure of $MoO_2Cl_2(bpym)$ [31].

The **violet** and **brown** species are mixtures of **1a** and **1b** in different proportions, based on the small energy difference between the two isomers (2 Kcal mol^{-1}), and that the bands observed in FTIR spectra (977 and 943 cm^{-1}) perfectly match those calculated for each complex, at 980 and 950 cm^{-1}. The weak absorption of the band at 943 cm^{-1} in the FTIR spectrum of the violet species lead us to associate it with a mixture with higher proportion of isomer **1a**, as the color is mainly dictated by the intensity of the band at 977 cm^{-1}, originated in the stretching of the Mo=O bond (length = 1.69 Å). Higher proportion of **1b** in the **brown** species is responsible for the increased intensity of the 943 cm^{-1} band. The ν(Mo=O) values are in good agreement with those reported for related complexes.

Relatively little is known of the spectroscopic properties of dinuclear $[Mo_2O_3]^{4+}$ (μ-oxo) complexes and $[Mo_2O_4]^{2+}$ (μ-dioxo). The vibrational spectra of Mo(V)

Table 2. Selected calculated and observed infrared and Raman spectral data (cm^{-1}).

Compounds	Calculated *trans*	Calculated *cis*	FTIR	Raman	Assignments
$MoOCl_3$ (**violet**)	980		977 s	976m	νMo=O
			943 sh	950 w	νMo=O
				381 m	νMo–Cl
				368	νMo–Cl
				317 w	νMo–N
$MoOCl_3$ (**brown**)	950		977 s	976 w	νMo=O
			943 m	950 w	νMo–Cl
				381 m	νMo–Cl
				368	νMo–N
				317 w	
$Mo_2O_3Cl_4(bpym)_2$ (**violet**)	969	976/973	966 s	963 m	νMo=O
	701	690/667	801 m	a	ν_{asym}Mo–O–Mo
				a	
	466	457	463–457 m	a	δMo–O–Mo
	414	409	414 m		ν_{sym}Mo–O–Mo
				366 w	νMo–Cl
$Mo_2O_4Cl_2(bpym)_2$ (**orange**)				317 vw	νMo–N
	950	963/940	955 s	954 m	νMo=O
			934 sh	934 w	ν_{asym}Mo–O_2–Mo
	720	735/608	735 m	–	
			499 – 486		δMo–O_2–Mo
			432		ν_{sym}Mo–O_2–Mo
				381 m	νMo–Cl
				368	νMo–Cl
				317 w	νMo–N
$Mo_2O_2Cl_6(\mu$-bpym) (**brown**)	991[b]	973[c]	983 s	974 w	νMo=O
	973[d]	959[e]	951 m	950 w	νMo=O
	336[b]			387 m	νMo–Cl
	336[b]			317 w	νMo–N

[a]The baseline Raman spectrum for $Mo_2O_3Cl_4(bpym)_2$ was not good.
[b,c]The oxo ligands are in the same bpym plane.
[d,e]The oxo ligands are out of the bpym plane.

dinuclear complexes containing the $[Mo_2O_3]^{4+}$ (μ-oxo) moiety show IR bands at $\sim$970 cm^{-1} for ν(Mo=O) and $\sim$750–800 cm^{-1} for ν_{as}(Mo–O–Mo). A third band at $\sim 430 \pm 25$ cm^{-1} has been attributed to either a ν_s(Mo–O–Mo) mode or to a deformation of the bridge [25].

The infrared spectrum of $Mo_2O_3Cl_4(bpym)_2$ shows only a strong band at 966 cm^{-1} assigned to Mo=O. In the Raman spectrum this band is observed at 963 cm^{-1}. The FTIR spectrum also has a medium band at 801 cm^{-1}, probably due to ν_{as}(Mo–O–Mo). A split band at 463–458 is assigned to bridge deformation, δ(Mo–O–Mo), whereas a band at 416 cm^{-1} is probably due to ν_s(Mo–O–Mo). The reported assignments are based on those previously made by Lincoln *et al.* [25].

The μ-oxo dimer consists of two distorted octahedral $MoOCl_2(bpym)$ units bridged by an oxo. Calculations found two isomers of similar energy for the $Mo_2O_3^{4+}$ (μ-oxo) dinuclear complexes, differentiated by the relative orientations of the Mo=O groups. In both cases the Mo=O bond lengths (1.69 and 1.71 Å) are similar to those found for other Mo(V) structures. The structure of **2a** is characterized by a linear Mo–O_b–Mo symmetric bridge with a 179.94° bond angle and a 1.87 Å Mo–O_b bond length (figure 1).

Bpym and oxo are located in the same plane. In **2b**, the oxo groups are *cis* with Mo=O distances of 1.69 Å. The optimized geometry shows a non-symmetric and nonlinear Mo–Ob–Mo bridge (bond angle 168.21°), with bpym defining a dihedral angle of 37.65°. The *trans* isomer is 2.77 kcal more stable than the *cis*.

The calculated vibrational spectra for the *trans* isomer shows Mo=O stretching at 969 cm^{-1}, the ν_{as}(Mo–O–Mo) at 701 cm^{-1}, and δ(Mo–O–Mo) at 466 and 414 cm^{-1}. The *cis* isomer has split bands, ν(Mo=O) stretching is calculated as a split band at 976 and 973 cm^{-1}, whereas ν_{as}(Mo–O–Mo) appears as two bands at 690 and 667 cm^{-1}, and the δMo–O–Mo as two bands at 457 and 409 cm^{-1}. According to the calculation, we associate $Mo_2O_3Cl_4(bpym)_2$ complex with **2a** having Mo=O groups *trans*. Isomer **2a** is centrosymmetric with only the symmetric mode (ν_s) Raman active and the antisymmetric mode (ν_{as}) is infrared active. Accordingly, the FTIR spectrum shows a strong band at 966 cm^{-1} (theoretical at 969 cm^{-1}) and at 963 cm^{-1} in the Raman spectrum, due to the symmetric vibration. The FTIR band at 966 cm^{-1} is in agreement with those reported for $Mo_2O_3Cl_4(dpy)_2$ (966 cm^{-1}) [32] and *trans* $Mo_2O_3Cl_4(HB(pz)_3)_2$ [25]. An additional band at 801, which is absent in the IR spectra of the mononuclear complexes, may be assigned to the ν_{as}(Mo–O–Mo) mode. This band is calculated at 701 cm^{-1}. We associate the mismatch between theoretical and experimental data, only found for ν_{as}(Mo–O–Mo), to a packing effect present in the *trans* isomer from interactions between bpym moieties. This effect shifts the ν_{as}(Mo–O–Mo) frequency in response to the increase of electron density of the aromatic ligands. The non-bonded interactions are not taken into account in the calculations "*in vacuo*." Nevertheless, it is well known that, in the solid, the environment affects the electron-donating and accepting properties of the ligand. In agreement with our results, a recent structural characterization of molybdenum(V) species [33] reports a band at 803 cm^{-1} for ν_{as}(Mo–O–Mo) bridge of the dimeric species mono-oxo $[Mo_2O_3Cl_6(H_2O)_2]^{2-}$. Other observed bands in the FTIR spectra, at 457 and 414 cm^{-1}, are assigned to δ(Mo–O–Mo) vibrations (calculated 466 and 414). These bands are characteristic of the dinuclear species with the linear or nearly linear Mo–O–Mo bridge [26–34], showing good agreement with theoretical results. Bands at 457, 414 and 801 cm^{-1} are absent in the monomeric species.

In the di μ oxo dimeric complexes, $Mo_2O_4Cl_2(bpym)_2$, the infrared spectrum shows a strong band at 955 cm^{-1} with a shoulder at 934 cm^{-1} that can be assigned to terminal Mo=O vibrations. The Raman spectrum also shows these at 954 and 934 cm^{-1}. The band in the Mo_2O_2 bridge at 735 cm^{-1} is due to the antisymmetric Mo–O_b stretch. A broad medium split band appears as peaks at 499 and 486 cm^{-1}, associated with δ and ν_s(Mo–O–Mo) modes, respectively. These features are not observed in the Raman spectrum. The assignments are consistent with those made for dioxo bridged species in complexes of Mo(V), $Mo_2O_4Br_2(Phen)_2$ [26] and $Na_2[Mo_2O_2(\mu\text{-}O)_2(cys)_2]\cdot 5H_2O$ [35].

The geometry optimization converged to two stable isomers for the dioxo complex in figure 1 (**3a** and **3b**). The *trans* form is centrosymmetric with a symmetric dioxo bridge and equal Mo=O bond lengths (1.71 Å). In the *cis* form, the two bpym ligands are almost perpendicular to each other, showing different Mo=O distances and an asymmetric dioxo bridge.

The calculated IR bands for the *trans* isomer have Mo=O stretching at 950 cm^{-1} and asymmetric Mo–O_2–Mo bridge at 720 cm^{-1}. The *cis* isomer displays split bands at 963/940 cm^{-1} for Mo=O and 735/608 cm^{-1} for the Mo_2O_2 bridge.

Both the calculated IR bands and relative energies point to the *trans* isomer as the dioxo complex experimentally observed. The shoulder observed at 934 cm^{-1} is probably

due to dipole- dipole coupling between the ν_{asym} Mo=O modes of the Mo=O groups, which are close to each other in the *trans* dimer (Mo–Mo distance of 2.57 Å *versus* 3.11 Å in the *cis* isomer). The relative energy calculated for the two isomers favors the *trans* isomer by 9 kcal mol^{-1} over the *cis*.

For bpym complexes, infrared spectra differentiate terminal or bridged bpym coordination. Two bands exist for terminal coordination, a sharp and characteristic band at 1656 cm^{-1} associated with another at 1580 cm^{-1} [36], and only one for a bridged bpym with the band at lower frequency not existing in bridge coordination. In the complexes analyzed herein, the IR spectra of **1**, **violet** and **brown**, **2**, and **3** show two bands associated with terminal bpym. The IR spectrum of **4** displays a unique band at 1580 cm^{-1}, indicative of bridged bpym.

The FTIR spectrum of $Mo_2O_2Cl_6(\mu$-bpym) shows two bands for Mo=O stretching, the most intense band located at 983 cm^{-1} and a medium band at 951. In the Raman spectrum these bands appear at 974 and 950 cm^{-1} with low intensity, very similar to those of the monomeric complexes.

The geometry optimization converged to four stable isomers for the bpym-bridged complexes (**4a**, **4b**, **4c** and **4d** in figure 1), two with oxo ligands in the same bpym plane (**4a** *trans* and **4b** *cis*) are 21 kcal mol^{-1} more stable than **4c** *trans* and **4d** *cis*. In the last two isomers, the Mo=O groups are axial relative to the bpym plane. The calculations indicate that *trans* **4a** and *cis* **4b** have slightly shorter Mo=O distance (1.682 Å) than **4c** and **4d** (1.696 Å). In the four isomers the bpym is in the same plane as the equatorial chlorides.

The calculated vibrational spectra for the four isomers show Mo=O stretching at 991, 973, 973 and 959 cm^{-1} for **4a**, **4b**, **4c** and **4d**, respectively.

Attending the experimental bands observed for $Mo_2O_2Cl_6(\mu$-bpym), we associate the 983 cm^{-1} band to **4a** (calculated at 991 cm^{-1}), and at 951 cm^{-1} to the **4d** isomer (calculated at 959 cm^{-1}) where the oxo groups are axial relative to the bpym plane.

In all the cases, the Mo–Cl and Mo–N stretching modes are only observed in the Raman spectrum due to the range in the FTIR (500 cm^{-1}).

The FTIR and Raman results for all complexes are shown in table 2, together with theoretical results.

Infrared results are in good agreement with theoretical calculations indicating the presence of *trans* and *cis* isomers (**violet** and **brown**) for the monomeric species. In the dimeric μ oxo the only band assigned to the Mo=O stretching indicates *trans* $Mo_2O_3Cl_4(bpym)_2$. For $Mo_2O_4Cl_2(bpym)_2$ the spectroscopic and theoretical results confirm *trans* isomer with Mo=O groups coupled due to the short distance between them (2.57 Å). The results found for the bpym-bridged complex support the presence of two isomers, **4a** and **4d**.

3.4. *Thermal analysis*

The complexes were studied in oxygen to 900°C. The characteristic peaks of the DTA curves are indicated in table 3. At 300–500°C the decomposition of complexes occurs with formation of MoO_3, characterized by infrared spectroscopy. This decomposition process has weak and poorly defined endothermic peaks in the DTA curves at 300–400°C and a remarkable exothermic peak in the 400–490°C range, due to total decomposition of the ligand.

Elimination of MoO_3 takes place at 750–800°C, through an endothermic peak.

Table 3. Significant peaks in the DTA curves of all the complexes.

Compounds	Exothermic peak (°C)	Endothermic peak (°C)
$MoOCl_3$ (**violet**)	485	791
$MoOCl_3$ (**brown**)	457	788
$Mo_2O_3Cl_4(bpym)_2$	437	771
$Mo_2O_4Cl_2(bpym)_2$	420	780
$Mo_2O_2Cl_6(\mu\text{-bpym})$	441	789

3.5. *Magnetic and EPR results*

The magnetic results from 4.6–290 K are summarized in table 4.

The **violet** and **brown** monomers have room temperature magnetic moments (1.60 and 1.61 MB) corresponding to Mo(V), lower than the spin only moment because of spin-orbit coupling. Plots of the corrected molar magnetic susceptibility per Mo(V), χ_M *versus* temperature for the **brown** complex are shown in figure 2. The **violet** compound is similar. The χ_M is approximately constant from 290–25 K. Below this temperature χ_M decreases, indicating an antiferromagnetic effect. Curie–Weiss fitting of the experimental data, according to the expression $\chi = C/(T-\theta)$ with plots of $\chi - 1$ *versus* T, have been used to estimate the θ values (figure 2). Fitting in the high temperature range ($T > 30$ K) gives a good linear correlation with θ values of -4.43 and -3.60 K for the violet and brown compounds, respectively. Higher temperatures have been used for **4** ($T > 70$ K) to ensure a proper extrapolation of the Curie-Weiss temperature, leading to a value of $\theta = -14.78$ K (figure 3).

The data were further fitted to a Curie law modified by inclusion of intermolecular interaction [37],

$$\chi = \frac{[Ng^2\beta^2 S(S+1)]}{[3kT - zJS(S+1)]}$$

where N, g, β, k and T have the usual meanings, J is the interaction parameter between two nearest neighbor paramagnetic species, z is the number of nearest neighbors around a given paramagnetic species in the crystal lattice and $S = 1/2$. The resulting zJ values, $-3.2\,cm^{-1}$ (**violet**) and $-3.0\,cm^{-1}$ (**brown**), correspond to an antiferromagnetic interaction.

For **2**, with a Mo–O–Mo bridge, the room temperature magnetic moment is 0.6 MB and decreases with decreasing temperature, common in compounds containing $[Mo_2O_3]^{4+}$ with a linear Mo–O–Mo bond, due to the interaction between the two Mo(V) atoms through the bridging oxygen, which leads to spin-pairing of the two unpaired electrons. As indicated by Garner *et al.* [38], the terminal oxygens are usually *cis* to the oxo bridge and *cis* or *trans* to each other. The d_{xy} orbital of Mo(V), with the unpaired electron, are in proper alignment with a p orbital on the bridging oxygen to form three-center molecular orbitals. The bonding and nonbonding orbitals are filled and the paired electrons give a diamagnetic structure. The magnetic behavior confirms the linear Mo–O–Mo bridge in **2**. Bending of the Mo–O–Mo bridge would lead to paramagnetism.

Table 4. Magnetic results for $MoOCl_3(bpym)$ (**1**) **violet** and **brown**, $Mo_2O_3Cl_4(bpym)_2$ (**2**) and $Mo_2O_2Cl_6(\mu\text{-bpym})$ (**4**) complexes.

Compound	θ^a (K)	$\mu(MB)^b$(290 K)	$\mu(MB)^b$ (4.6 K)	g	zJ^c (cm^{-1})	J^d (cm^{-1})	ρ^d	R($\times 10^4$)
1 (violet)	−4.43	1.60	1.29	1.94[c]	−3.2			6.89
1 (brown)	−3.60	1.61	1.33	1.95[c]	−3.0			3.08
2		0.6						
4	−14.78	1.20	0.63	1.95[d]		−10.1	0.03	8.62

[a]From the Curie–Weiss law, $\chi = C/(T-\theta)$, more details in the text.
[b]Magnetic moment per Mo(V) atom.
[c]From intermolecular interaction equation.
[d]From intramolecular interaction equation.
$R = \Sigma_i[(\chi_M)_{obs}(i) - (\chi_M)_{calc}(i)]^2/\Sigma_i[(\chi_M)_{obs}(i)]^2$.

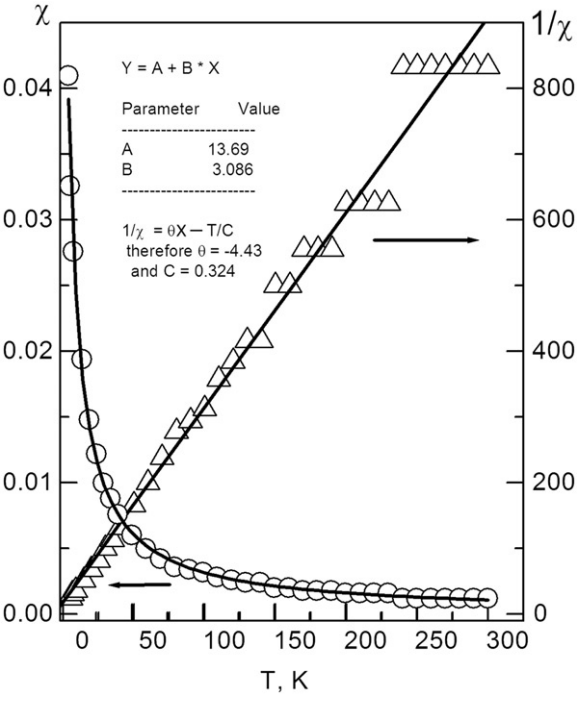

Figure 2. Plots of $\chi_M(cm^3\ mol^{-1})$ *vs.* T and $1/\chi_M$ *vs.* T for $MoOCl_3(bpym)$ (**1b**). Solid line shows the best fit indicated in the text.

For **4**, the magnetic moment decreases with decreasing temperature. The plot of magnetic susceptibility per dimer *versus* temperature (figure 3) indicates a significant antiferromagnetic intradimer interaction. The data were fitted using the Bleaney-Bowers equation for dimers with $S_1 = S_2 = 1/2$ modified by inclusion for monomeric impurity [39]:

$$\chi = C\ 2\exp(2x)(1-\rho)/[1+3\exp(2x)] + C\rho/2$$

where $C = Ng^2\beta^2/kT$, $x = J\,(kT)^{-1}$ and $\rho =$ fraction of monomeric impurity. The J value, $-10.1\,cm^{-1}$, corresponds to antiferromagnetic coupling. In general, bipyrimidine generates a weak antiferromagnetic exchange between paramagnetic cations.

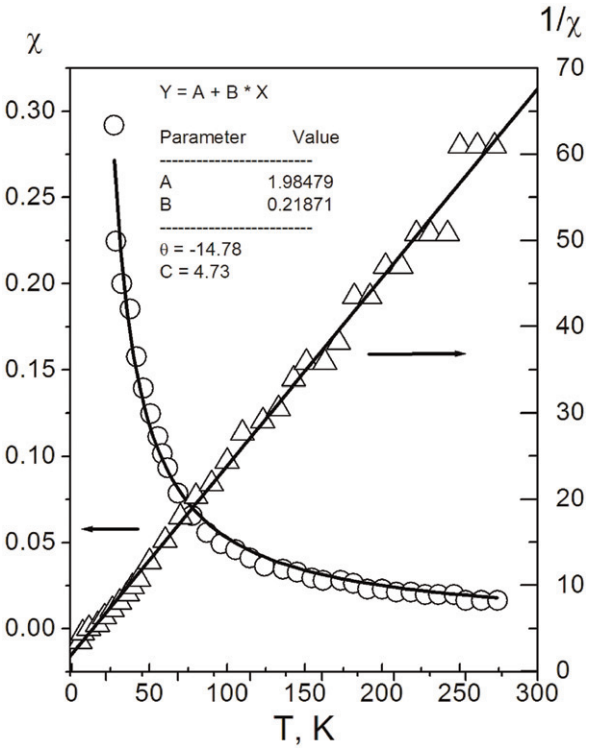

Figure 3. Plots of χ_M ($cm^3\ mol^{-1}$) *vs.* T and $1/\chi_M$ *vs.* T for $Mo_2O_2Cl_6(\mu\text{-bpym})$ (**4**). Solid line shows the best fit indicated in the text.

The antiferromagnetic interaction observed in bpym-bridged dimers of divalent first-row transition metal ions has been explained by σ overlap in the plane between the $d_{x^2-y^2}$ orbital of each metal ion and the HOMO of bpym. In the case of Cu(II) this is the only operative exchange pathway because only the $d_{x^2-y^2}$ orbital may be occupied by the unpaired electron [40, 41]. In other metal ions the π-exchange pathway is operative but makes negligible contribution. For Mo(V), with a $4d^1$ electron configuration, the antiferromagnetic interaction must be attributed to the π-exchange pathway because the unpaired electron cannot be located in the $d_{x^2-y^2}$ orbital. Expansion of the 4d orbitals in comparison with that of the 3d orbitals may be significant given the absence of magnetic interaction in $[(VO)_2Cl_4(\mu\text{-bpym})]$, with a $3d^1$ electron configuration.

The powder spectra (Q band) at 290 and 100 K for **violet** and **brown** are similar with a symmetric signal ($g = 1.95$). For **4** an orthorhombic signal is recorded at different temperatures, with $g_1 = 1.97$, $g_2 = 1.94$ and $g_3 = 1.93$.

4. Conclusions

$MoOCl_3$(bpym) (violet and brown), $Mo_2O_3Cl_4(bpym)_2$, $Mo_2O_4Cl_2(bpym)_2$ and $Mo_2O_2Cl_6(\mu\text{-bpym})$ were synthesized and characterized by elemental analyses,

thermogravimetry and FTIR, Raman and EPR spectroscopy. The chemistry is further demonstration of the propensity for molybdenum(V) to hydrolyze with formation of different isomers and dimers. Theoretical calculations for **1**–**4** provide a comparison spectroscopic and structural data for the monomeric and dimeric species. The calculated geometries are in good agreement with experimental determinations reported for related compounds and can be nicely correlated with the spectroscopic data. The agreement between observed and calculated vibrational data allows further assignment of the synthesized complexes.

References

[1] G. Wilkinson (Ed.), *Comprehensive Coordination Chemistry*, Vol. 3, p. 1347, Pergamon Press, Oxford (1987).
[2] J. Selbin. *Angew. Chem., Int. Ed.*, **5**, 712 (1966).
[3] H.K. Saha, M.C. Halder. *J. Inorg. Nucl. Chem.*, **33**, 3719 (1971).
[4] B. Spivack, Z. Dori. *Coord. Chem. Rev.*, **17**, 99 (1975).
[5] E. Carmona, A. Galindo, L. Sánchez, A.J. Nelson, G. Wilkinson. *Polyhedron*, **3**, 347 (1984).
[6] E.I. Stiefel. *Prog. Inorg. Chem.*, **22**, 1 (1977).
[7] J.H. Enemark. *J. Am. Chem. Soc.*, **113**, 9193 (1991).
[8] H.K. Saha, M.C. Halder. *J. Inorg. Nucl. Chem.*, **33**, 3719 (1971).
[9] A.V. Butcher, J. Chatt. *J. Chem. Soc. A*, 2652 (1970).
[10] L. Manojlovic-Muir, K.W. Muir. *J. Chem. Soc., Dalton Trans.*, 686 (1972).
[11] J.H. Enemark. *J. Am. Chem. Soc.*, **113**, 9193 (1991).
[12] A. Bashall, S.W.A. Bligh, A.J. Edwards, V.C. Gibson, M. McPartlin, O.B. Robinson. *Angew. Chem., Int. Ed. Engl.*, **31**, 1607 (1992).
[13] E. Martínez de la Hidalga, M. Barquín, M.J. González Garmendia. *An. Quím.*, **87**, 781 (1991).
[14] M. Barquin, M.J. González Garmendia, V. Bellido. *Transition Met. Chem.*, **24**, 546 (1999).
[15] M. Barquin, M.J. González Garmendia, V. Bellido. *Transition Met. Chem.*, **24**, 584 (1999).
[16] M.J. Frisch, G.W. Trucks, H.B. Schlegel, G.E. Scuseria, M.A. Robb, J.R. Cheeseman, J.A. Montgomery, Jr, T. Vreven, N. Kudin, J.C. Burant, J.M. Millam, S.S. Iyengar, J. Tomasi, V. Barone, B. Mennucci, M. Cossi, G. Scalmani, N. Rega, G.A. Petersson, H. Nakatsuji, M. Hada, M. Ehara, K. Toyota, R. Fukuda, J. Hasegawa, M. Ishida, T. Nakajima, Y. Honda, O. Kitao, H. Nakai, M. Klene, X. Li, J.E. Knox, H.P. Hratchian, J.B. Cross, V. Bakken, C. Adamo, J. Jaramillo, R. Gomperts, R.E. Stratmann, O. Yazyev, A.J. Austin, R. Cammi, C. Pomelli, J.W. Ochterski, P.Y. Ayala, K. Morokuma, G.A. Voth, P. Salvador, J.J. Dannenberg, V.G. Zakrzewski, S. Dapprich, A.D. Daniels, M.C. Strain, O. Farkas, D.K. Malick, A.D. Rabuck, K. Raghavachari, J.B. Foresman, J.V. Ortiz, Q. Cui, A.G. Baboul, S. Clifford, J. Cioslowski, B.B. Stefanov, G. Liu, A. Liashenko, P. Piskorz, I. Komaromi, R.L. Martin, D.J. Fox, T. Keith, M.A. Al-Laham, C.Y. Peng, A. Nanayakkara, M. Challacombe, P.M.W. Gill, B. Johnson, W. Chen, M.W. Wong, C. Gonzalez, J.A. Pople. *Gaussian 03, Revision C.02, Gaussian, Inc.*, Pittsburgh, PA (2003).
[17] A.D. Becke, D.R. Yarkony. In *Modern Electronic Structure Theory Part II*, World Scientific, Singapore (1995).
[18] W.J. Bassis Hehre, L. Radom, P.V.R. Schleyer, J.A. Pople. *Ab Initio Molecular Orbital Theory*, John Wiley & Sons, New York (1986).
[19] (a) P.J. Hay, W.R. Wadt. *J. Chem. Phys.*, **82**, 270 (1985); (b) W.R. Wadt, P.J. Hay. *J. Chem. Phys.*, **82**, 284 (1985); (c) P.J. Hay, W.R. Wadt. *J. Chem. Phys.*, **82**, 299 (1985).
[20] (a) D.L. Harris. *Curr. Opin. Chem. Biol.*, **5**, 724 (2001); (b) L. Noodleman, T. Lovell, W.-G. Han, J. Li, F. Himo. *Chem. Rev.*, **104**, 459 (2004); (c) E.I. Solomon, R.K. Szilagyi, S. DeBeer, G.L. Basumallick. *Chem. Rev.*, **104**, 419 (2004); (d) G. Estiu, K.M. Merz, Jr. *J. Phys. Chem. B*, **111**, 10263 (2007).
[21] A. Scott, L. Radom. *J. Phys. Chem.*, **100**, 16502 (1996).
[22] A.B. Blake, F.A. Cotton, J.S. Wood. *J. Am. Chem. Soc.*, **86**, 3024 (1964).
[23] J.R. Knox, C.K. Proust. *Acta Crystallogr., Sect. B Struct. Crystallogr.; Cryst. Chem.*, **B25**, 2281 (1969).
[24] C.K. Proust, C. Couldwell. *Acta Crystallogr., Sect. B Struct. Crystallogr.; Cryst. Chem.*, **B36**, 1481 (1980).
[25] S. Lincoln, T. Loehr. *Inorg. Chem.*, **29**, 1907 (1990).
[26] H.K. Saha, A.K. Bernejee. *J. Inorg. Nucl. Chem.*, 1872 (1972).
[27] S.E. Lincoln, S.A. Koch. *Inorg. Chem.*, **25**, 1594 (1986).

[28] F.W. Moore, M.L. Larson. *Inorg. Chem.*, **6**, 998 (1967).
[29] C.J. Ballhausen, H.B. Gray. *Molecular Orbital Theory*, Benjamin, New York (1965).
[30] P.C.H. Mitchell. *J. Inorg. Nucl. Chem.*, **25**, 963 (1963).
[31] E. Fritz Kühn, M. Groarke, É. Bencze, E. Herdtweck, A. Prazeres, A.M. Santos, M.J. Calhorda, C.C. Romão, I.S. Gonçalves, A.D. Lopes, M. Pillinger. *Chem. Eur. J.*, **8**, 2370 (2002).
[32] F.A. Cotton, D. Hunter. *J. Coord. Chem.*, **3**, 359 (1974).
[33] F. Jalilehvand, V. Mah, B.O. Leung, D. Ross, M. Parvez, R.F. Aroca. *Inorg. Chem.*, **46**, 4430 (2007).
[34] R. Aguado, J. Escribano, M.R. Pedrosa, A. De Cian, R. Sanz, F.J. Arnaiz. *Polyhedron*, **26**, 3842 (2007).
[35] N. Ueyama, M. Nakata, T. Araki, A. Nakamura, S. Yamashita, T. Yamashita. *Inorg. Chem.*, **20**, 1934 (1981).
[36] M. Julve, M. Verdaguer, J.A. Real, G. Bruno. *Inorg. Chem.*, **32**, 795 (1993).
[37] O. Kahn. *Molecular Magnetism*, p. 26, Wiley VCH Publisher Inc., USA and Canada (1993).
[38] C.D. Garner, J.M. Charnock. In *Comprehensive Coordination Chemistry*, G. Wilkinson (Ed.), Vol. 3, p. 1347, Pergamon Press, Oxford (1987).
[39] M. Nakashina, M. Mikuriya, Y. Muto. *Bull. Chem. Soc. Jpn*, **58**, 968 (1985).
[40] M. Julve, G. Munno, G. Bruno, M. Verdaguer. *Inorg. Chem.*, **27**, 3160 (1988).
[41] G. Munno, G. Viau, M. Julve, F. Lloret, J. Faus. *Inorg. Chim. Acta*, **257**, 121 (1997).